

Relating statistics to dynamics in axisymmetric homogeneous turbulence

Fabien S. Godeferd^a

^aLMFA CNRS UMR 5509, École Centrale de Lyon, Université de Lyon, France
36 avenue Guy de Collongue F-69131 Écully
E-mail: fabien.godeferd@ec-lyon.fr

Abstract

The structure and the dynamics of homogeneous turbulence are modified by the presence of body forces such that the Coriolis or the buoyancy forces, which may render a wide range of turbulence scales anisotropic. The corresponding statistical characterization of such effects is done in physical space using structure functions, as well as in spectral space with spectra of two-point correlations, providing two complementary viewpoints. In this framework, second-order and third-order structure functions are put in parallel with spectra of two-point second- and third-order velocity correlation functions, using passage relations. Such relations apply in the isotropic case, or for isotropically averaged statistics, which, however, do not reflect the actual more complex structure of anisotropic turbulence submitted to rotation or stratification. This complexity is demonstrated in this paper by orientation-dependent energy and energy transfer spectra produced in both cases by means of a two-point statistical model for axisymmetric turbulence. We show that, to date, the anisotropic formalism used in the spectral transfer statistics is especially well-suited to analyze the refined dynamics of anisotropic homogeneous turbulence, and that it can help in the analysis of isotropically computed third-order structure function statistics often used to characterize anisotropic contexts.

Keywords: Homogeneous turbulence. Anisotropy. Spectra. Structure functions.

1. Introduction

Homogeneous turbulence submitted to distortions such as solid body rotation, stratification, or the Lorentz force in the MHD context, exhibit axisymmetric statistics, as a clear departure from isotropy. These anisotropic effects that arise due to modified dynamics or energy exchange do not fall within the classical description of turbulence in Kolmogorov's theory. The following general questions, pertaining to the understanding of anisotropic homogeneous turbulence, can therefore be raised:

1. How can we characterize the anisotropy of the flow, at one or two point, in physical or spectral statistical descriptions?
2. Are passage relations available between: (a) the two-point statistics of structure functions, necessarily measured in physical space in experiments, and (b) kinetic energy and transfer spectra? (Which can be obtained for high Reynolds number turbulence from statistical models.)
3. How can we interpret the modified dynamics of anisotropic turbulence? (It can be observed in terms of anomalous scalings of energy spectra or energy transfer spectra readily available in two-point statistical models.)
4. Can we exploit some features easily accessed in spectral space to refine the phenomenological analysis of the dynamics of turbulence in physical space?
5. Do Kolmogorov scalings available for high Reynolds number isotropic turbulence apply to isotropically integrated statistics of anisotropic turbulence?
6. What level of complexity do we have to introduce to go beyond the mere isotropic description, *e.g.* starting with axisymmetric flows?

October 31, 2018

As a bootstrap, we start, hereafter in this introductory section, by reviewing a few of the existing works related to these issues, and introduce some of the existing results and formalism available in the statistical characterization of axisymmetric turbulence. In section 2, we describe the relationships available for isotropic turbulence for second- and third-order statistics appearing in both Lin's and Kármán-Howarth's equations, and suggest to extend the description of the velocity increment statistics to the anisotropic case, and to relate them to the modified dynamics in axisymmetric homogeneous turbulence, especially energy and transfer spectra. Results for the latter, in the case of stably stratified or rotating turbulence, are provided in section 4.1. We choose to use an anisotropic two-point statistical model, described shortly in section 3, since it permits to reach higher Reynolds number and smoother statistics than direct numerical simulation. Assuming isotropized passage relations, we then derive second- and third-order velocity structure functions, presented in section 4.2, and discuss the results against existing scalings for isotropic turbulence.

The spectral formalism for homogeneous turbulence allows to remove altogether the role of pressure, and hence permits a highly refined analysis of the dynamics of anisotropic turbulence, and on its sources; for instance from the role of inertial waves interactions in rotating turbulence, or for the dynamics of stably stratified turbulence in which the transfers are split between internal waves and potential vorticity interactions. Even in flows which are thought to be isotropic, in experimental or numerical realizations, a degree of anisotropy may be hidden, depending on how the characterization of the isotropy of the flow has been done: the isotropy of *rms* velocity components or of integral length scales only characterizes the large scales, whereas vorticity or dissipation can be used for the smaller ones. The computation of anisotropic spectra allows to quantify such scale-dependent level of isotropy, or anisotropy, and to isolate the most important energy transfer contributions. Alternately, the statistics in physical space do not easily permit the removal of pressure from balance equations, and thus prevent from a tractable access to modal decompositions (*e.g.* the

toroidal/poloidal decomposition). It however applies to locally inhomogeneous flows, which is not easily accessible to spectral analysis. We therefore emphasize the importance of both spectral and physical viewpoints, and the fact that they are *complementary*, which we expose and discuss in this paper, taking rotating or stably stratified turbulence as supporting evidences.

In what follows in this section, we review a few studies which have been devoted to the characterization of anisotropy in turbulence, from the point of view of directional statistics in physical space — including both anisotropy of velocity components or dependence on the separation vector — and studies about the anisotropic spectral scalings in anisotropic turbulence, related to the dynamics of the flow.

If initially isotropic, homogeneous turbulence can be rendered anisotropic by introducing an external distortion on the flow: solid body rotation is present for instance in geophysical flows and acts through the Coriolis force, as well as a buoyancy force in density- or temperature- stratified layers. In conducting fluids, the action of an external magnetic field also modifies the symmetries by means of the Lorentz force. In these three examples, the intensity of the corresponding force depends on the orientation of the fluid motion with respect to either the rotation axis, the gravity axis, the background magnetic field axis. Wave propagation can also be present, *e.g.* inertio-gravity waves or Alfvén waves. They provide an anisotropic way of redistributing energy in terms of scale and direction, such that the dynamics of energy exchange in the turbulence is strongly modified. We focus here on the effects of solid body rotation and stable density stratification on homogeneous turbulence.

Studies about anisotropic turbulence were proposed and stemmed from various preoccupations. The theory of axisymmetric turbulence was regarded as a logical extension to the theory of isotropic turbulence, and was developed by Batchelor [1] — in which parallel and perpendicular directions (with respect to the axis of symmetry) were distinguished to express statistical quantities, *e.g.* the dissipation — and by Chandrasekhar [2] in the 50s. In these studies, the imposed symmetries do not account for the possible presence of helicity, unlike the extension

proposed by Lindborg about the kinematics of axisymmetric turbulence [3]. More recently, some exact vectorial laws were also proposed by Galtier for rotating homogeneous turbulence, exposing the need for a transverse/longitudinal components distinction (with respect to the separation vector) when computing velocity structure functions [4]. An extensive discussion and review of the anisotropy in turbulent flows was proposed by Biferale & Procaccia [5] using the symmetry group analysis (SO(3) for Navier-Stokes equations). These authors discuss Kolmogorov's theory and how to relate anisotropic flows to the n -th order structure functions, especially looking at the 4/5 law for the third-order one, which includes the isotropy hypothesis.

On the one hand, the structure-function approach has recently been used for an experimental characterization of rotating turbulence dynamics by Lamriben *et al.* [6], and for mesoscale turbulence in the atmosphere by Lindborg & Cho [7], both works including a discussion of the level of anisotropy to account for, as a departure to classical Kolmogorov scalings of velocity increments moments. In an experimental study concerning a turbulent jet, Xu & Antonia [8] emphasize the importance of discriminating between the longitudinal and transverse velocity components when expressing the structure function in axisymmetric turbulence, and Oyewola *et al.* use structure functions to describe the anisotropy of the small scales in a turbulent boundary layer [9]. In situ experiments by Kurien *et al.* in the atmospheric boundary layer also permitted to exhibit the different scalings of the structure functions, distinguishing between longitudinal and transverse increments, by separating the lowest order anisotropy contributions thanks to the SO(3) symmetry group. [10]

On the other hand, several efforts were devoted to establishing the scalings that should apply to two-point velocity correlation spectra depending on the perpendicular k_{\perp} or the parallel k_{\parallel} wavenumber components with respect to the axis of symmetry. In the geophysical context, one may retrieve atmospheric spectra as in rotating strongly stratified turbulence. At small scales (several kilometers), Kolmogorov $k_{\perp}^{-5/3}$ scaling is retrieved, whereas at large scales (several hundreds of kilome-

ters), depending on the velocity component considered the scaling is either k_{\perp}^{-3} (zonal wind) or k_{\perp}^{-2} (meridional wind). [11] In the context of conducting fluids, plasmas and astrophysics, Galtier has also proposed several spectral scalings with spectra of the form $k_{\perp}^{-\alpha} k_{\parallel}^{-\beta}$ to account for anisotropy in magnetohydrodynamic turbulence [12]. However, the physical arguments available for discussing the anisotropy of conducting fluid submitted to the Lorentz force are not available for disentangling the intricate nonlinear dynamics of rotating turbulence, and, to some extent of stably stratified turbulence.

In most of the above-mentioned works, spectra are used to characterize the cascade of energy and the dynamics of anisotropic turbulence, or structure functions compared with the isotropic theory scalings. Very few works are devoted to the relationship between the two formalisms, and the current paper is a first attempt at providing *quantitative* information on how anisotropic spectra dynamics can be used to interpret physical space velocity increment statistics.

Thus, taking into account the modifications of the turbulence structure and dynamics due to external effects can be done at different levels. The statistical description of the velocity field can be done at a two-point level in physical space by the second-order velocity correlation tensor $R_{ij}(\mathbf{r}) = \langle u_i(\mathbf{x})u_j(\mathbf{x}+\mathbf{r}) \rangle$ where \mathbf{r} is the separation vector. Fourier-transforming this tensor yields the spectrum tensor $\Phi_{ij}(\mathbf{k}) = 1/(8\pi)^3 \int R_{ij}(\mathbf{r}) \exp(-i\mathbf{k} \cdot \mathbf{r}) d\mathbf{r}$, whose trace is $\Phi_{ii}(\mathbf{k}) = E(k)/2\pi k^2$ in isotropic turbulence, with $k = |\mathbf{k}|$ and $E(k)$ is the kinetic energy spectrum. Kolmogorov theory supports the scaling $E(k) \sim k^{-5/3}$ in isotropic turbulence at high Reynolds number.

However, external distortions render the turbulent flow statistics dependent on the orientation of \mathbf{r} in physical space, *e.g.* for the two-point correlations $R_{ij}(\mathbf{r})$. In isotropic turbulence, this tensor depends only on two scalar function, namely the longitudinal two-point correlation function $f(r)$, and the transverse one $g(r)$ [13], and is expanded over the tensors δ_{ij} and $r_i r_j / r^2$. In axisymmetric turbulence, which is the case we consider here—where the axis of symmetry \mathbf{n} is borne by the rotation vector in rotating turbulence or the axis of gravity in stably stratified

turbulence—, $R_{ij}(\mathbf{r})$ depends on four scalars and requires the addition of the two expansion tensors $r_i n_j / r$ and $n_i n_j$ [1].

The anisotropic dependence of the two-point correlation tensor in turn translates into a dependence of the corresponding spectra $\Phi_{ij}(\mathbf{k})$ on the orientation θ of the wavevector \mathbf{k} with respect to the axis of symmetry \mathbf{n} (the latter is the same as in physical space). The spectra can similarly also be decomposed in a general way over four scalars (see *e.g.* [14] and [15]).

This correspondence between the physical space two-point statistical formalism of turbulence and the spectral description not only applies to second-order correlation tensors and spectra, but it also extends to third-order statistics, and moreover to velocity structure functions. The latter are of great use in Kolmogorov's description of isotropic turbulence, and are described *e.g.* in [16] and in [17]. Considering the velocity increment $\delta\mathbf{u} = \mathbf{u}(\mathbf{x} + \mathbf{r}) - \mathbf{u}(\mathbf{x})$, in the isotropic context one commonly computes the n^{th} -order structure function $\langle\langle(\delta u)^n\rangle\rangle$ based on the longitudinal projection u of the velocity vector onto the separation vector \mathbf{r} . The brackets indicate averaging using statistical homogeneity. Obviously, when turbulence is anisotropic, one should also distinguish different components in the structure functions and different orientations of \mathbf{r} , although most of the theoretical results are available only in the isotropic context. One of them is the exact Kolmogorov four-fifth law wherein the third-order structure function $D_{LLL}(r) = \langle\langle(\delta u)^3\rangle\rangle = -4/5\varepsilon r$, valid for r in the inertial subrange, where ε is the averaged dissipation [18], or, in a different form proposed by Antonia *et al.* [19]:

$$\langle\delta u(\delta u_j \delta u_j)\rangle = -\frac{4}{3}\varepsilon r. \quad (1)$$

where repeated indices imply summation.

In the following, we investigate how anisotropic turbulence can recover the above scalings, using the two-point statistical EDQNM model. The question about the convergence of the statistics of the structure functions to the 4/5 limit has been addressed before. Antonia & Burattini studied this limit at increasing Reynolds numbers [20], and it appears that the convergence is very slow, and may not be yet reached in the existing

experiments. However, this low-Reynolds number effects has to be separated from the anisotropic effect in non isotropic flows. The leading order small-scales K41 scalings may be recovered in anisotropic flows, provided suitable filtering has been applied to the data, as shown with DNS fields by Taylor *et al.* [21]. In the following, the interpretation of the scaling laws provided by EDQNM results therefore mixes the isotropic small-scales turbulent behavior with the anisotropic contributions, since no such separation as in Taylor *et al.* has been made.

2. The link between spectral dynamics and velocity structure functions

The above-mentioned structure functions provide a scale-dependent statistical characterization of turbulence with a two-point separation. It is clear that they are related to the two-point correlation functions, *and their spectral counterparts*, such that second-order velocity structure functions are related to two-point velocity correlation spectra, and third-order structure functions to energy transfer spectra (triple velocity correlations at two points).

In the anisotropic context, and when dealing with statistically axisymmetric turbulence, the orientation θ of the Fourier vector \mathbf{k} with respect to the axis of symmetry borne by \mathbf{n} , has to be taken into account, so that an additional dependence has to be introduced in the energy spectrum: $E(k, \theta)$. Integrating the latter over $\theta \in [-\pi, \pi]$ of course provides an equivalent spherically averaged $E(k)$. At this stage, the question of the resulting inertial scaling of the spectrum is raised.

The kinetic energy spectrum $E(k)$ and the nonlinear energy transfer spectrum $T(k)$ appear in the Lin equation as

$$\partial_t E(k) + 2\nu k^2 E(k) = T(k) \quad (2)$$

in the isotropic case, where ν is the viscosity, such that the total dissipation is $\varepsilon = 2\nu \int k^2 E(k) dk$. In the rotating case for instance, phase-scrambling anisotropically changes the shape of the energy exchange term $T(k, \theta)$ in an equation equivalent to (2) (see next equation 11). The transfer contains third-order correlation terms, and is thus related to the third-order statistics

that are used to quantify nonlinearity such as the skewness of velocity gradient.

Regarding second-order moments, one can obtain second-order structure functions starting with the two-point correlation spectra. For instance,

$$\langle(\delta u_i \delta u_i)\rangle = 2 \int_0^\infty \left(1 - \frac{\sin kr}{kr}\right) E(k) dk . \quad (3)$$

where repeated indices are summed, contains information from all the velocity components.

Equation (2) therefore relates the evolution of second-order statistics—the energy spectrum—to third-order ones—the transfer. The analogous in physical space of (2) is the Kármán-Howarth equation

$$\partial_t (u'^2 f) = \left(\partial_r + \frac{4}{r}\right) [R_{LLL}(r, t) + 2\nu \partial_r (u'^2 f)] \quad (4)$$

in which $f(r)$ is the longitudinal two-point correlation function; the longitudinal two-point third-order correlation function is $R_{LLL}(r, t) = \langle u_i(\mathbf{x}, t) u_m(\mathbf{x}, t) u_i(\mathbf{x} + \mathbf{r}, t) \rangle r_m / r$, $r = |\mathbf{r}|$, and $(3/2)u'^2$ is the total kinetic energy. Upon examining (2) and (4) together, it is clear that if the dynamics of turbulence is anisotropic, one might expect not only a different equilibrium between the dissipative and nonlinear related terms of these equations, and a directional dependence with \mathbf{k} of the Lin equation for $E(\mathbf{k})$ transposed into anisotropy with respect to \mathbf{r} in the Kármán-Howarth equation. The derivation of the latter equation relies on assumption of isotropy, but the general Kármán-Howarth-Monin equation, which contains the same terms that depend on the separation *vector* \mathbf{r} can be derived as (see Frisch [17], p. 78 for a derivation, and *e.g.* [6]):

$$\frac{1}{2} \frac{\partial}{\partial t} \langle \mathbf{u}(\mathbf{x}) \mathbf{u}(\mathbf{x} + \mathbf{r}) \rangle = \frac{1}{4} \nabla \cdot \langle \delta \mathbf{u}(\mathbf{r}) |\delta \mathbf{u}(\mathbf{r})|^2 \rangle + \nu \nabla^2 \langle \mathbf{u}(\mathbf{x}) \mathbf{u}(\mathbf{x} + \mathbf{r}) \rangle \quad (5)$$

The dependence of the velocity, or velocity increments $\delta \mathbf{u}$, on the direction of \mathbf{r} with respect to \mathbf{n} , is therefore an important parameter in axisymmetric turbulence statistics. For isotropic turbulence, Kolmogorov's theory (1941) only considers a scalar longitudinal increment δu , provides the scaling $\langle(\delta u)^n\rangle \sim (\varepsilon r)^{n/3}$, and allows to draw from equation (4) a simplified relationship between second- and third-order structure

functions

$$\langle(\delta u)^3\rangle = -\frac{4}{5} \varepsilon r + 6\nu \partial_r \langle(\delta u)^2\rangle.$$

which yields, at infinite Reynolds number, the famous four fifths law

$$\langle(\delta u)^3\rangle = -(4/5)\varepsilon r, \quad (6)$$

or equation (1). [19]

A useful relationship can be established between third-order spectral statistics *i.e.* the nonlinear energy transfer $T(k)$, and the third-order structure function :

$$\langle \delta u (\delta q)^2 \rangle = 4r \int_0^\infty g(kr) T(k) dk \quad (7)$$

where $g(kr) = (\sin kr - kr \cos kr)/(kr)^3$ and $(\delta q)^2 = (\delta u_i \delta u_i)$. It shows the direct link of the third-order structure function on the dynamics of turbulence.

Formulas similar to equations (3) and (7) rigorously derived for anisotropic turbulence are still not available in the general case, but, in the rotating case, the isotropic relationships apply, since the Coriolis force is not a production term in the balance equations, and drops out altogether in the isotropized balance equations, both in physical and spectral spaces. In general anisotropic turbulence, the analogous of (7) implies a vector dependence of the structure functions on \mathbf{r} . It also shows that a dynamics modified by an external distortion applied to homogeneous turbulence translates immediately in a modification of the structure functions. It is therefore interesting to discuss the applicability of Kolmogorov scalings in flows that contain some anisotropy. Attempts at such scalings for rotating turbulence are proposed by Galtier [4], or by Lindborg & Cho using atmospheric data. [7] In the axisymmetric case, an extensive work is in progress [22].

3. Statistical model for the spectral anisotropy of axisymmetric turbulence

We study a simplified case which nonetheless captures some important anisotropic physical mechanisms in *e.g.* geophysical flows: stable stratification and rotation, taken into account in the

Boussinesq system of equations for an incompressible fluid:

$$\partial_t \mathbf{u} + \mathbf{u} \cdot \nabla \mathbf{u} - \nu \nabla^2 \mathbf{u} = -\nabla p - 2\Omega \mathbf{n} \times \mathbf{u} + b \mathbf{n}, \quad (8)$$

$$\partial_t b + \mathbf{u} \cdot \nabla b - \chi \nabla^2 b = -N^2 \mathbf{n} \cdot \mathbf{u}, \quad (9)$$

$$\nabla \cdot \mathbf{u} = 0, \quad (10)$$

where b is the buoyancy field, associated with fluid density fluctuations around background density augmented by mean density gradient. N is the Brunt-Väisälä (buoyancy) frequency and Ω the rotational frequency. The corresponding terms, Coriolis force and buoyancy force, act on the velocity field linearly and compete against the nonlinear advection term. In this study, the separate effects of either one is considered (although the combination of both characterizes some atmospheric or oceanic flows, with a ratio $\alpha = 2\Omega/N \sim 1/10$).

In rotating or stratified turbulence, the dynamics of the flow is superimposed with wave-like motion that transfers energy differently from the classical turbulent dynamics. In the linear limit, at large N or Ω , one recovers wave turbulence, as a soup of superimposed inertial waves or internal gravity waves. For instance, “turbulence” and “wave” like dynamics may be defined by splitting the velocity field in the eigenmodes of the linearized system (8)–(10), so that the total turbulent energy of a rotating and stratified flow can be divided into a “vortex” mode and a “wave” mode. The linear evolution of the wave mode is governed by the dispersion relation $\sigma(\mathbf{k}) = N \sin \theta$ for internal waves and $\sigma(\mathbf{k}) = 2\Omega \cos \theta$ for inertial waves, which depend on θ , the polar angle with the vertical, whence a directional dependence of the turbulent motion.

In order to study relatively high Reynolds number turbulence, we introduce a statistical model which describes the evolution of the two-point correlation spectra, whose dynamical equations derive from (8)–(10), introducing a closure known as EDQNM. The Eddy-Damped Quasi-Normal Markovian model for isotropic turbulence was studied by several authors (see *e.g.* Orszag [23]) decades ago, although it has recently regained interest for its ability to reach very high Reynolds numbers as demonstrated by the spectrum we computed with EDQNM, shown on figure 1. (Similar figures are presented in [24].)

The more advanced version developed for rotating or stably stratified turbulence (denoted EDQNM₂ since it differs significantly from the model for isotropic turbulence) reflects more accurately the wave dynamics and is capable of taking into account anisotropic features. In the limit of very strong rotation, for instance, it becomes identical to the wave turbulence closures described by Zakharov [25], although in this book, Zakharov *et al.* do not consider anisotropic dispersion relations as for instance inertial waves. An extensive description of the EDQNM₂ closure model is provided in [26, 14], as well as comparisons with Direct Numerical Simulations (DNS) and Large Eddy Simulations (LES) which show a very good agreement and illustrate the capability of the model to accurately represent anisotropic turbulence. We find that, among other closures, only the EDQNM₂ model for closing the spectral transfer terms (the equivalent to T in equation 2) was capable of predicting all the anisotropic features observed in the DNS and LES results. The model equations for the generalized transfer terms, *e.g.* $T^e(\mathbf{k})$ for the directional kinetic energy spectrum, involve sums of eight contributions (according to polarities of triadic interactions), weighted by the rotation-dependent factor (or Brunt-Väisälä frequency in the stratified case):

$$T^e = \sum_{\epsilon, \epsilon', \epsilon'' = \pm 1} \int_{\mathbf{k} + \mathbf{p} + \mathbf{q} = 0} \frac{\mathbf{S}_{kpq}^e(\text{QN})}{\vartheta_{kpq}^{\epsilon, \epsilon', \epsilon''}} d^3 \mathbf{p} \quad (11)$$

The numerator of the integrand takes into account the quasi-normal expansion for non-isotropic turbulence and is closed in terms of quadratic combinations of the two-point correlation spectra, whereas the denominator involves viscous and eddy-damping effects through

$$\vartheta_{kpq}^{\epsilon, \epsilon', \epsilon''} = \vartheta_{kpq} (1 + 2i\vartheta_{kpq}\Omega(\epsilon k_{\parallel}/k + \epsilon' p_{\parallel}/p + \epsilon'' q_{\parallel}/q)) \quad (12)$$

for a triad of wavevectors $\mathbf{k} + \mathbf{p} + \mathbf{q} = 0$ with polarities $\{\epsilon, \epsilon', \epsilon''\} = \{\pm 1\}^3$, thus accounting for the explicit linear rotation effects on triple correlation through the phases. Thus, the classical timescale ϑ_{kpq} in the isotropic non-rotating case is replaced by the preceding triadic complex timescales. As already mentioned, the above expression is consistent with wave turbulence results [27, 28]. The isotropic EDQNM model consists only of the Lin equations (2) in which the transfer term is

closed using double products of energy spectra $E(k)$, and where the only dependence variable is the wavenumber k .

4. Second- and third-order structure functions derived from spectral statistics

The EDQNM₂ model for rotation and stable stratification consists of equations for the two-point correlation spectra similar to (2) in which the nonlinear transfer spectra in the right-hand-side are replaced by their closure. In the model for rotating turbulence, four coupled equations are solved for the energy density spectrum $e(\mathbf{k})$, the helicity $h(\mathbf{k})$ and the polarization spectra $Z(\mathbf{k})$, each of which is expressed at each discretized spectral point in the polar-spherical representation of wavevectors \mathbf{k} , that is as functions of discretized (k, θ) :

$$\begin{aligned} \left(\frac{\partial}{\partial t} + 2\nu k^2\right)e &= T^e \\ \left(\frac{\partial}{\partial t} + 2\nu k^2 + 4i\Omega\frac{k_3}{k}\right)Z &= T^z \\ \left(\frac{\partial}{\partial t} + 2\nu k^2\right)h &= T^h \end{aligned} \quad (13)$$

The transfer spectra are also discretized in the same way.

For stratified turbulence, the density spectrum of rescaled potential energy $\Phi_3(\mathbf{k})$ and the cross-correlation spectrum for density and velocity $\Psi(\mathbf{k})$ are involved

$$\begin{aligned} \left(\frac{\partial}{\partial t} + 2\nu k^2\right)\Phi_1 &= T^1 \\ \left(\frac{\partial}{\partial t} + 2\nu k^2\right)(\Phi_2 + \Phi_3) &= T^2 + T^3 \\ \left(\frac{\partial}{\partial t} + 2\nu k^2 - 2iN \sin \theta_k\right)(\Phi_2 - \Phi_3 + i\Psi_R) &= T^2 - T^3 + IT^{\Psi_R} \end{aligned} \quad (14)$$

along with the kinetic energy spectrum decomposed in poloidal and toroidal spectra $\Phi_2(\mathbf{k})$ and $\Phi_1(\mathbf{k})$.

Equations (13) and (14) are therefore generalized versions of the Lin equation (2) and are exact equations, unless a closure such as equation (11) is applied. Moreover, in both systems (13) and (14), the decomposition of the spectra is optimized to yield simple and meaningful equations: the Z equation in (13) contains the oscillatory part due to the effect of rotation, and the last equation of (14) represents oscillations due to the

kinetic/potential energy exchange, mediated by the flux Ψ produced by buoyancy.

The complexity of these systems of equations and anisotropic damping (12) provided by the EDQNM₂ model needs to be contrasted with the simplicity of the EDQNM model for $E(k)$ whose dynamical equation is only (2).

The corresponding set of time-dependent differential equations are advanced in time starting from initial conditions which correspond to a narrow-band distribution of kinetic energy centered about a prescribed peak. The spectra then evolve into developing an inertial subrange and a dissipative one. From this time on, turbulence evolves in a self-similar decay.

The evolved rotating turbulence spectrum presented on figure 1 corresponds to a Reynolds number $Re = 7000$ and the Rossby number is $Ro = u/(\Omega L) = 0.04$ (u is the *rms* velocity, L the integral scale and Ω the rotation rate) although the figures at initial time were higher, since they usually decay in time. For the stratified turbulence spectrum, $Re = 1000$ and the Froude number is $Fr = u/(NL) = 0.09$, where N is the Brunt-Väisälä frequency which characterizes the intensity of the vertical density gradient. Note that the Reynolds number is lower in the stratified simulation, since a part of the dynamics is contained in the potential energy stored by density fluctuations around the mean density.

4.1. Quick comments on the spectral statistics and the dynamics of anisotropic turbulence

The developed spectra for isotropic, rotating, and stably stratified turbulence are plotted on figure 1. Note that spectra of anisotropic turbulence, in our model, but also in DNS or in experimental measurements, depend on the orientation of the wavevector, in agreement with two-point correlation functions which depend on the orientation of the separation vector. The relevant parameter is the angle θ with the axis of symmetry.

We have purposefully chosen an very high Reynolds number for the isotropic spectrum for three reasons: (a) it demonstrates the capacity of statistical EDQNM closures to reach Reynolds numbers closer to those observed in geophysical or astrophys-

ical contexts than is possible with DNS; (b) the anisotropic EDQNM₂ closure requires additional computational effort, and therefore the inertial ranges observed on the corresponding spectra of figure 1 span roughly two decades and are reduced with respect to the isotropic case; however, equivalent DNS would require an order of magnitude larger computational effort; (c) although the isotropic EDQNM spectrum exhibits six decades of inertial subrange, the corresponding kinetic energy transfer plotted on figure 2 only exhibits a narrow plateau at zero (if at all) between the energy-losing large scales and the energy-gaining small dissipative scales, also corresponding to constant downscale spectral energy flux.

One should also note that statistical two-point models are by essence better adapted to produce smooth spectral statistics than Direct Numerical Simulations. First, the discretization of the spectral space can be adapted easily when solving EDQNM equations, by adjusting both the wavenumber k distribution and its orientations, with the possibility of accumulating grid points towards the equatorial or the polar directions. By construction, DNS is constrained to a Cartesian uniform grid discretization of Fourier components. Moreover, the recent experiment by Lamriben *et al.* [6] has shown that ensemble averaging requested to compute smooth third-order statistics — namely third-order structure functions or energy transfers — required hundreds of realizations, an issue which also applies to DNS realizations. Since the statistical two-point model equations already concern the statistics of the second- and third-order moments, explicit ensemble averaging is self-contained in the model (as observed in the following smooth figures of results produced by EDQNM).

The structure of decaying rotating turbulence has been described extensively from experimental [29], theoretical, and numerical results [14, 30]. Inertial wave turbulence was studied by Galtier [31], and Mininni & Pouquet investigated energy and helicity spectra of rotating turbulence [32], with different spectral scaling for each. The dynamics and modified energy cascade produce an anisotropic structure which was simulated with high resolution DNS also by Morinishi *et al.* [33]. Anomalous

scaling of structure functions in rotating turbulence also permitted Seiwert *et al.* to investigate the intermittency of rotating turbulence [34].

The interpretation of the dynamics leading to rotating homogeneous turbulence structuration is still debated; the two main viewpoints rely either on linear timescales of inertial waves, with the Coriolis force acting on locally inhomogeneous structures that emit waves [35], or on a long-term nonlinear effect [14]. It is not the object of this paper to reconcile these viewpoints, but, in short, both agree that in rotating turbulence vortices are elongated along the axis of rotation. The corresponding dynamics is that of preferential energy transfer towards motion close to two-dimensional, although complete two-dimensionalization is not expected. It also means that energy accumulates in orientation dependent kinetic energy spectra $E(k, \theta)$ in the vicinity of the two-dimensional manifold $\theta \simeq \pi/2$ which is the neighborhood of horizontal wavevectors in spectral space. This is confirmed by the angular dependent energy spectrum plotted on the top panel of figure 3, which also compares well with spectra processed from DNS of decaying rotating turbulence. Note that the power-law scaling of the corresponding spectrum in figure 1 is the result of the spherical averaging over the directional spectra of figure 3, with no single identical power-law applying to each individual one. The bottom panel of figure 3 presents a tentative measure of the anisotropy in the spectra, by subtracting to the directional spectral the averaged spectrum. The curves present only the limit spectra, equatorial or polar; also note that the anisotropy is *reversed* between the rotating and the stratified cases, with more energy in the polar direction (along the symmetry axis) in stratified turbulence, whereas the accumulation of spectral energy in rotating turbulence is in the vicinity of the equatorial (perpendicular to the symmetry axis) direction.

For the stably stratified case, the spectral structuration is reversed, such that the energy accumulates in spectra of vertical \mathbf{k} ($\theta \simeq 0$) as shown on figure 3 (see also *e.g.* Lindborg [11]). Again, the anisotropic statistical model compares extremely well with experimental wind-tunnel observations and

DNS [26]. These comparisons not only concern dynamical quantities, such as energy or dissipation, but also directional integral length scales, and the most refined possible comparison between directional spectra $E(k, \theta)$, that is for every direction of every scale. In both the stratified and the rotating cases, EDQNM₂ model predictions are very close to the same spectral statistics extracted from DNS fields, down to the most refined ones. In physical space, the structuration of stably stratified turbulence corresponds to a layering of the flow, with strong horizontal motion, and vanishing vertical velocity, although the flow retains a strong vertical *variability* due to the presence of large vertical gradients $\partial/\partial z$. [36, 37]

The anisotropy observed in the spectra of figure 3 is the departure of each spectrum $E(k, \theta)$ around the average shown on figure 1. Since the plot is in logscale, the clear difference between horizontal wavenumber spectra and vertical ones demonstrates the large ratio between the energy in vertical and horizontal motion. Moreover, one observes that in the stratified turbulence spectrum the anisotropy is largest at the larger, energy-containing, scales, although it extends to the middle of the inertial sub-range; in the rotating turbulence spectrum, the anisotropy extends throughout the inertial range down to the smallest scales. Of course, this observation depends on the values of the Rossby and Froude numbers as well as on the Reynolds number. The rotation (or stratification) timescale has to be compared to the local timescale of a given turbulent structure associated with wavenumber k in order to assess whether its dynamics may be affected by the Coriolis or the Boussinesq forces (for instance by computing a Zeman scale $(\Omega^3/\epsilon)^{-1/2}$ [38], where ϵ is the dissipation, or similarly an Ozmidov scale for stratified turbulence by replacing Ω by N [39]). It nonetheless demonstrates that there exist parameter ranges at which turbulence may be strongly affected by external distortions, and its structure and dynamics can depart significantly from that of isotropic turbulence.

In addition to providing the second-order statistics corresponding to the two-point energy spectra discussed above, the closure provides quantitative information on third-order two-

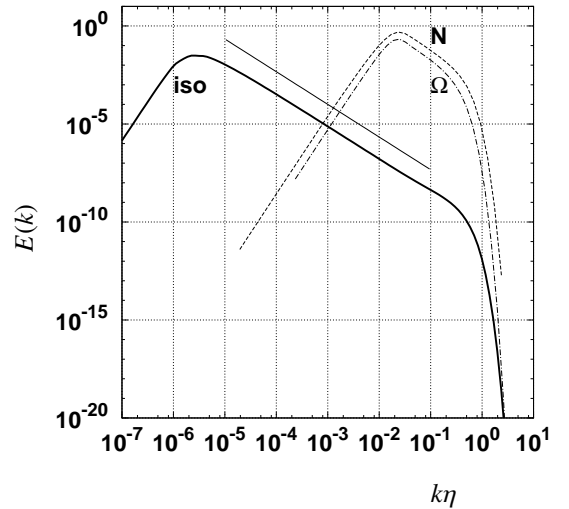


Figure 1: Solid line: Kinetic energy spectrum $E(k)$ of isotropic turbulence at $Re^L = 26 \times 10^6$ given by the EDQNM closure model. Dot-dashed line: spherically accumulated kinetic energy spectrum given by the EDQNM₂ model for rotating turbulence. Dashed line: spectrum given by the closure for stratified turbulence. The inertial range $k^{-5/3}$ power-law is also shown on the figure, corresponding to the scaling of the isotropic spectrum. The spectra for rotating and stratified turbulence both scale like $k^{-1.9}$. The wavenumber k is normalized by the inverse of the Kolmogorov length scale η .

point correlation spectra, *i.e.* the kinetic energy transfer spectra shown on figure 2. Apart from the Reynolds number difference, the spherically averaged transfer spectra of anisotropic turbulence are similar to the isotropic turbulence transfer. Note that we present spectra of the kinetic energy transfer $T^e(k)$, which is only a part of the energy transfers occurring in stratified turbulence, since there is also coupling with the potential energy mode. As observed in the isotropic case, in the anisotropic cases energy is drawn from the large scales and injected in the small scales in a classical forward cascade. In the meantime, if one observes the orientation-dependent transfer spectra (not presented here), one also notices a re-distribution of energy among different orientations of wavevectors, even at constant wavenumber, *i.e.* without interscale exchange.

4.2. Structure functions

The above observations of second- and third-order correlations spectra have a direct impact on the second- and third-order structure functions of turbulence, according to the dual-

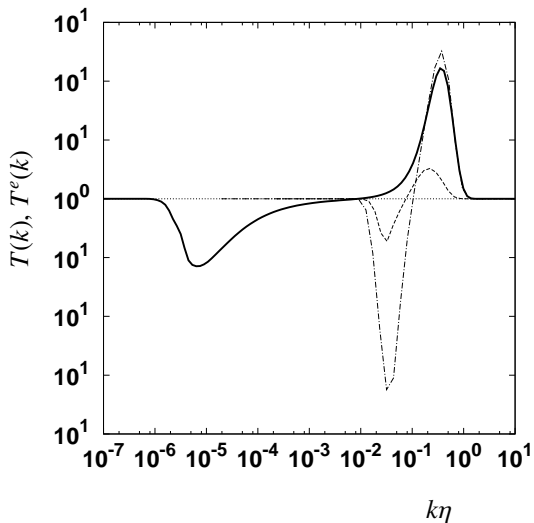


Figure 2: Solid line: Kinetic energy transfer spectrum $T(k)$ of isotropic turbulence given by the EDQNM closure model (scaled by 10^2 to render it visible). Dot-dashed line: spherically accumulated kinetic energy transfer spectrum $T^e(k)$ given by the EDQNM₂ model for rotating turbulence. Dashed line: transfer spectrum given by the closure for stratified turbulence.

ity of spectral and physical space. Some passage relations between the two spaces have been presented in section 2. We now present the results obtained by using these relations applied to the EDQNM closure results for isotropic and anisotropic turbulence. It is however not possible to derive any n^{th} -order structure function from spectral information contained in two-point statistical closures, precisely because the spectral information is restricted to n^{th} -order correlations at *two* points. A case-by-case inspection is thus required.

The relation (3) linking the kinetic energy spectrum to the second-order structure function is applied to the results obtained by EDQNM, and also to the anisotropic turbulence results. The numerical resolution of the isotropic EDQNM model directly provides discretized distribution of $E(k)$ and $T(k)$. For the EDQNM₂, the spherically averaged spectra $E(k)$ and $T(k)$ are obtained from the anisotropic spectral data $E(k, \theta)$ and $T^e(k, \theta)$, by averaging over θ . Once these data are obtained, a simple numerical quadrature of the integrals in equations (3) and (7) is used to obtain $\langle\langle \delta u_i \delta u_i \rangle\rangle$ and $\langle \delta u (\delta q)^2 \rangle$ (likewise for $\langle\langle \delta u \rangle^3 \rangle$ with an integral not recalled here). The corresponding structure function is normalized by $(\varepsilon r)^{2/3}$ and plotted against

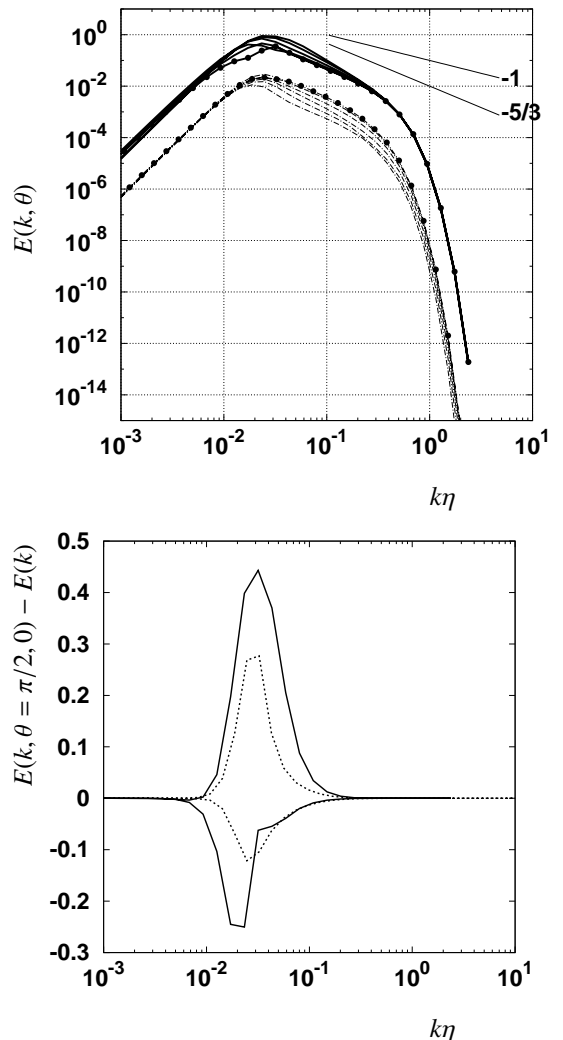


Figure 3: Top panel: Orientation-dependent kinetic energy spectra $E(k, \theta)$ (seen to be monotonically varying with θ). Solid lines: results from EDQNM₂ model for stratified turbulence; dashes: results from the EDQNM₂ model for rotating turbulence, shifted down one decade. For each case, a subset of the discretized orientations θ are presented. Spectra corresponding to horizontal wavevectors are indicated by black dots. Bottom panel: A measure of the anisotropy showing the difference between the polar and equatorial spectra with the spherically averaged one. Solid lines: EDQNM₂ result for stratified turbulence, dashed lines for the rotating results.

r/η (η is the Kolmogorov length scale) on figure 4, showing the scaling which is obtained for isotropic turbulence, and illustrating the advantage brought by achieving a high value of the Reynolds number. For rotating turbulence and for stably stratified turbulence, the corresponding values of the Reynolds number are lower, and one has to deal with a narrower curve. It is clear, however, that the isotropic scaling is far from being applicable to the anisotropic turbulence structure functions, since, here, if we compute $\max(\langle\langle\delta u_i\delta u_i\rangle\rangle)/(\varepsilon r)^{2/3}$, one obtains 3.4 for the isotropic case, 4.2 for the stratified case, 6.6 for the rotating case.

This is also observed on the curves for the third-order structure functions plotted on figures 5 and 6 in two different forms. Figure 5 shows the averaged cubed longitudinal increment $\langle(\delta u)^3\rangle$ divided by the behavior proposed in Kolmogorov theory: $-(\varepsilon r)$. The expected proportionality constant $4/5$ is clearly recovered by the EDQNM closure transfer processed through equation (6), with a nice plateau tangential to the $y = 4/5$ horizontal line. It should be noted that even at this very high value of the Reynolds number the extent of the plateau is less than a decade in scale. This may explain part of the early controversies about the precise value of the proportionality constant obtained from experimental measurements. The same considerations apply for the other form of the third-order structure function proposed by [19], $\langle\delta u(\delta u_j\delta u_j)\rangle$, with a proportionality constant $4/3$ with εr , plotted on figure 6 using equation (1). In both plots, the scaling is obviously not the right one for rotating turbulence or for stratified turbulence, although the order of magnitude of the peaks of the structure functions for the anisotropic turbulence cases are consistent with the isotropic turbulence one. ($\max(\langle\delta u(\delta u_j\delta u_j)\rangle)/(\varepsilon r)$ is marginally lower than 0.8 in the isotropic case, 0.39 for stratified results and 1.02 for the rotating results.)

In rotating turbulence, the energy cascade is known to be reduced by the presence of rotation, so that the dissipation is lower than for an equivalent Reynolds number isotropic turbulence dynamics. This can explain the fact that the peaks of $-\langle\delta u(\delta u_j\delta u_j)\rangle/(\varepsilon r)$ or of $-\langle(\delta u)^3\rangle/(\varepsilon r)$ are higher than in

isotropic turbulence. In addition, one observes on figures 5 and 6 a negative excursion of the third-order structure function in the very large scales, which could be attributed to a trend towards a reverse cascade, although this has to be confirmed by other simulations.

In the stratified case, the trend is reversed, an effect which could be attributed to augmented dissipation. The analysis is subtle here, since there is not only a cascade of energy due to classical nonlinear turbulent interaction, but there is also a coupling between the kinetic energy and the potential energy. It seems that the balance between energy taken away from the velocity field for creating density fluctuations is more than compensated by the increased dissipation from the added scalar cascade. An attempt at including the part of dissipation arising in the potential energy balance fails at correcting enough the scaling of the third-order structure functions of stratified turbulence in figures 5 and 6.

Finally, in order to address the Reynolds number dependence issue for the third-order structure function convergence, we computed an isotropic turbulence EDQNM result for a lower Reynolds number than proposed above, at $Re = 2600$, of the same order of magnitude as those for the anisotropic EDQNM₂ data. The solid curve of figure 5 shows the corresponding result, which underestimates significantly the $4/5$ constant. The departure amplitude is similar to that of the anisotropic data, although we believe it is of different nature. Following the analysis by Taylor *et al.* [21], there are therefore two sources of departure to the K41 scaling, one due to low Reynolds number effect, the other to anisotropy. Here, for the anisotropic runs, anisotropy is responsible for the departure from the asymptotic large Reynolds number scaling, since for rotating turbulence it leads to an *overestimate*, whereas for stratified turbulence it is *underestimated*. Also, the measures presented by Antonia & Burattini for isotropic turbulence exhibit a uniform convergence from *below* the value $4/5$ [20]. Thus, although there may be a finite Reynolds number effect, we believe that, to first order, the difference with the high Reynolds number isotropic scaling is due to anisotropy. This argument is also supported by the curve

for the second-order structure function in isotropic turbulence at the lower Reynolds number $Re = 2600$ presented on figure 4. It shows that although the asymptotic large Reynolds number scaling of is not yet reached, the maximum of $\langle(\delta u_i \delta u_i)\rangle/(\epsilon r)^{2/3}$ is within 30% of the asymptotic value, whereas the peak for rotating turbulence is twice this value. The shape of the spectra and the difference in the downscale cascading rate in the anisotropic runs with respect to the isotropic one can only explain this departure.

5. Conclusion and perspectives

We have described in this work the spectral statistics of anisotropic turbulence, with spectra of second- and third-order two-point correlations. These kinetic energy spectra and kinetic energy transfer spectra are the result of the spherical averaging of spectra of correlations taken with separations along different angles with respect to the axis of symmetry, or in other words for different orientations of the wavevectors. Not only these angle-dependent spectra correspond to variable intensities of the energy, but their inertial range scaling, when averaged, produces the power-law scaling of the overall kinetic energy spectrum. Results obtained by a two-point statistical closure of EDQNM type show that, at high Reynolds number, the resulting anisotropy can be strong, and corresponds to a non classical structuration of the flow. The cases of strongly rotating turbulence and strongly stratified turbulence were investigated, with respectively an elongation of the vortices along the rotation axis or a horizontal layering. The velocity components are consequently of variable magnitude in the vertical and horizontal directions, so that an impact on the velocity second-order structure functions is expected. The access to the detailed energy transfers also permits the computation of third-order structure functions, and the comparison with exact scalings obtained for isotropic turbulence. As expected, the constants obtained are different, although thanks to the relationships presented in section 2 one is able to closely related the anisotropic spectral characterization to the structure functions, thus to link the dynamics of energy cascade and inter-orientation transfer to the statistical

moments in physical space. The departure from K41 theory for anisotropic turbulence statistics of the second- and third-order structure functions shows that the Kàrmàn-Howarth equation from which theoretical scalings are derived exhibits a modified equilibrium when the structure of turbulence is anisotropic. The correspondence with the Lin equation shows that the dynamics of anisotropic turbulence is also modified, and we are able to trace the origin of the modified energy spectra scalings to the transfer terms. Since these transfer terms are accessible by spectral theory, this may be a way to improve the prediction of the third-order structure function moment in rotating or stratified turbulence, using two-point statistical closures.

Of course, this calls for additional work and further developments, including the derivation of relationships equivalent to (3) and (1) but considering the specific components of velocity parallel or orthogonal to the axis of symmetry. In so doing, one will highlight the value of the anisotropic EDQNM₂ closure which not only allows to model high Reynolds number turbulence but also provides quantitative information on the anisotropy of statistics.

This work is funded by the French *Agence Nationale de la Recherche* under grant number ANISO-340803. The reviewing work and suggestions of the Referees is also thankfully acknowledged.

- [1] G. K. Batchelor, The theory of axisymmetric turbulence, Proc. R. Soc. Lond. A 186 (1007) (1946) 480–502.
- [2] S. Chandrasekhar, The theory of axisymmetric turbulence, Philosophical Transactions of the Royal Society of London. Series A, Mathematical and Physical Sciences 242 (855) (1950) 557–577.
- [3] E. Lindborg, Kinematics of homogeneous axisymmetric turbulence, J. Fluid Mech. 302 (1995) 179–201.
- [4] S. Galtier, Exact vectorial law for homogeneous rotating turbulence, Phys. Rev. E 80 (4) (2009) 046301. doi:10.1103/PhysRevE.80.046301.
- [5] L. Biferale, I. Procaccia, Anisotropy in turbulent flows and in turbulent transport, Physics Reports 414 (2-3) (2005) 43–164. doi:10.1016/j.physrep.2005.04.001.
- [6] C. Lamriben, P.-P. Cortet, F. Moisy, Direct measurements of anisotropic energy transfers in a rotating turbulence experiment, Phys. Rev. Lett. 107 (2011) 024503.
- [7] E. Lindborg, J. Cho, Horizontal velocity structure functions in the upper

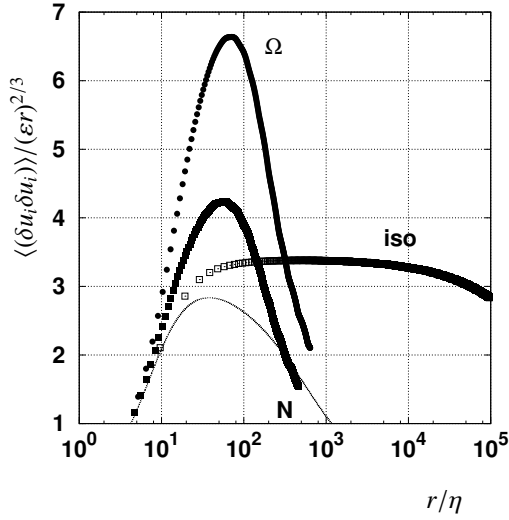


Figure 4: Second-order structure function $\langle(\delta u_i \delta u_i)\rangle$ computed from (3) normalized by $(\epsilon r)^{2/3}$ as a function of the separation r normalized by the Kolmogorov length scale η . Open squares: results from the EDQNM model for isotropic turbulence; Filled squares: results from EDQNM₂ model for stratified turbulence; Filled circles: results from EDQNM₂ model for rotating turbulence. The dotted line presents isotropic turbulence EDQNM results at $Re = 2600$.

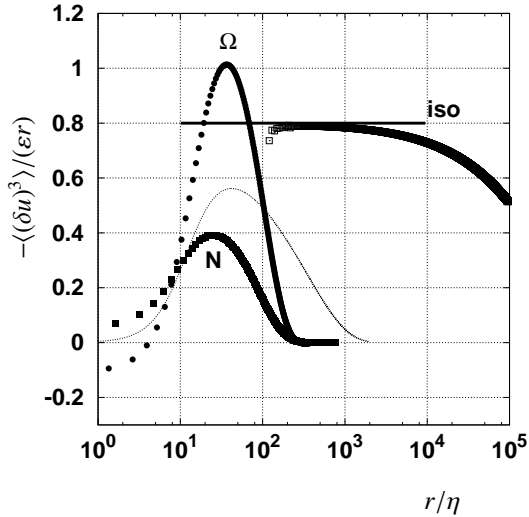


Figure 5: Third-order structure function of the longitudinal velocity increment $\langle(\delta u)^3\rangle$ normalized by $-(\epsilon r)$ as a function of the separation normalized by the Kolmogorov length scale. Same symbol convention as in figure 4. The horizontal line exhibits the 4/5 scaling. The dotted line presents isotropic turbulence EDQNM results at $Re = 2600$.

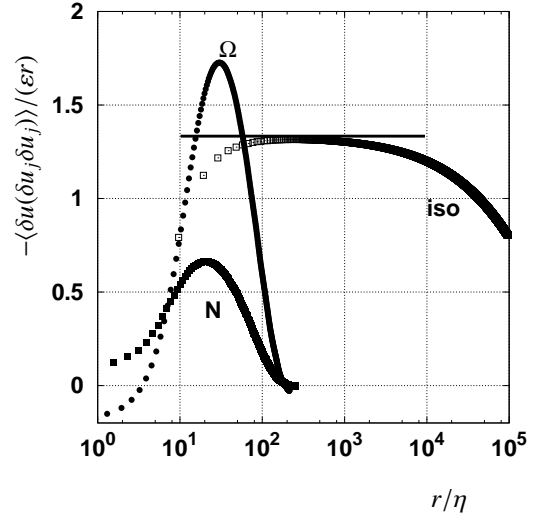


Figure 6: Third-order structure function $\langle\delta u(\delta u_j \delta u_j)\rangle$ as proposed by [19] normalized by $-(\epsilon r)$ as a function of the separation normalized by the Kolmogorov length scale. Same symbol convention as in figure 4. The horizontal line exhibits the 4/3 scaling.

troposphere and lower stratosphere. 2. theoretical considerations, *J. Geophys. Res.* 106 (D10) (2001) 233–241.

- [8] G. Xu, R. Antonia, S. Rajagopalan, Scaling of mixed longitudinal-transverse velocity structure functions, *Eur. Phys. Let.* 44001 (2007) 5 pages.
- [9] M. Oyewola, L. Djenidi, R. Antonia, Examination of anisotropy of the small-scale motion in a perturbed low Reynolds number turbulent boundary layer, *Exp. Therm. & Fluid Sci.* 32 (2007) 309–315.
- [10] S. Kurien, V. S. L'vov, I. Procaccia, K. R. Sreenivasan, Scaling structure of the velocity statistics in atmospheric boundary layers, *Phys. Rev. E* 61 (1) (2000) 407–421.
- [11] E. Lindborg, The energy cascade in a strongly stratified fluid, *J. Fluid Mech.* 550 (2006) 207–242.
- [12] S. Galtier, A. Pouquet, A. Mangeney, On spectral scaling laws for incompressible anisotropic magnetohydrodynamic turbulence, *Phys. Plasmas* 12 (2005) 092310.
- [13] G. Batchelor, *The theory of homogeneous turbulence*, Cambridge University Press, 1953.
- [14] C. Cambon, N. N. Mansour, F. S. Godeferd, Energy transfer in rotating turbulence, *J. Fluid Mech.* 337 (1997) 303–332.
- [15] P. Sagaut, C. Cambon, *Homogeneous turbulence dynamics*, Cambridge University Press, 2008.
- [16] A. Monin, A. Yaglom, *Statistical fluid mechanics*, Vol. 2, MIT Press (ed. J. Lumley), Cambridge, Mass., 1975.
- [17] U. Frisch, *Turbulence: The Legacy of A. N. Kolmogorov*, Cambridge University Press, 1996.
- [18] A. N. Kolmogorov, *The local structure of turbulence in incompressible*

- viscous fluid for very large reynolds numbers, *Dokl. Akad. Nauk. SSSR* 32 (16).
- [19] R. Antonia, M. Ould-Rouis, F. Anselmet, Y. Zhu, Analogy between predictions of kolmogorov and yaglom, *J. Fluid Mech.* 332 (1997) 395.
- [20] R. A. Antonia, P. Burattini, Approach to the 4/5 law in homogeneous isotropic turbulence, *J. Fluid Mech.* 550 (2006) 175–184.
- [21] M. A. Taylor, S. Kurien, G. L. Eyink, Recovering isotropic statistics in turbulence simulations: The kolmogorov 4/5th law, *Phys. Rev. E* 68 (026310).
- [22] C. Cambon, L. Danaila, F. Godeferd, J. Scott, Detailed anisotropy in the statistical description and dynamical approach to turbulent flows, *J. Fluid Mech.* submitted.
- [23] S. A. Orszag, Analytical theories of turbulence, *J. Fluid Mech.* 41 (1970) 363–386.
- [24] W. J. T. Bos, J. Bertoglio, Dynamics of spectrally truncated inviscid turbulence, *Physics of Fluids* 18 (7) (2006) 071701. doi:10.1063/1.2219766.
- [25] V. E. Zakharov, V. S. L’Vov, G. Falkovich, *Kolmogorov Spectra of Turbulence I: Wave Turbulence*, Springer-Verlag, 1992.
- [26] F. S. Godeferd, C. Staquet, Statistical modelling and direct numerical simulations of decaying stably stratified turbulence. part 2. large-scale and small-scale anisotropy, *Journal of Fluid Mechanics* 486 (2003) 115–159. doi:10.1017/S0022112003004531.
- [27] D. Benney, P. Saffman, Nonlinear interaction of random waves in a dispersive medium, *Proc. R. Soc. London Ser. A* 289 (1966) 301–320.
- [28] F. Bellet, F. S. Godeferd, J. F. Scott, C. Cambon, Wave turbulence in rapidly rotating flows, *Journal of Fluid Mechanics* 562 (2006) 83. doi:10.1017/S0022112006000929.
- [29] C. Morize, F. Moisy, M. Rabaud, Decaying grid-generated turbulence in a rotating tank, *Phys. Fluids* 17 (9) (2005) 095105.
- [30] K. Yoshimatsu, M. Midorikawa, Y. Kaneda, Columnar eddy formation in freely decaying homogeneous rotating turbulence, *Journal of Fluid Mechanics* 677 (2011) 154–178.
- [31] S. Galtier, Weak inertial-wave turbulence theory, *Phys. Rev. E* 68 (1) (2003) 015301. doi:10.1103/PhysRevE.68.015301.
- [32] P. Mininni, A. Pouquet, Helicity cascades in rotating turbulence, *Phys. Rev. E* 79 (2009) 026304.
- [33] Y. Morinishi, K. Nakabayashi, S. Q. Ren, Dynamics of anisotropy on decaying homogeneous turbulence subjected to system rotation, *Physics of Fluids* 13 (10) (2001) 2912. doi:10.1063/1.1398040.
- [34] J. Seiwert, C. Morize, F. moisy, On the decrease of intermittency in decaying rotating turbulence, *Phys. Fluids* 20 (2008) 071702.
- [35] P. J. Staplehurst, P. A. Davidson, S. B. Dalziel, Structure formation in homogeneous, freely decaying, rotating turbulence, *J. Fluid Mech.* 598 (2008) 81–103.
- [36] K. Yoon, Z. Warhaft, The evolution of Grid-Generated turbulence under conditions of stable thermal stratification, *Journal of Fluid Mechanics* 215 (1990) 601–638. doi:10.1017/S0022112090002786.
- [37] O. Praud, A. M. Fincham, J. Sommeria, Decaying grid turbulence in a strongly stratified fluid, *Journal of Fluid Mechanics* 522 (2005) 1–33. doi:10.1017/S002211200400120X.
- [38] P. Mininni, D. Rosenberg, A. Pouquet, Two small-scale inertial ranges in rotating helical turbulence and the return to isotropy, submitted. URL <http://arxiv.org/abs/1104.5519v1>
- [39] R. Ozmidov, Vertical exchange in the ocean, *Physical Oceanography* 9 (1999) 417–425. doi:10.1007/BF02524658.